FORM TI-12
8/94

WAPD-T-3122

CONF-970488--2

LABORATORY GALLING TESTS OF SEVERAL COMMERCIAL COBALT-FREE HARDFACING ALLOYS

B. V. COCKERAM, R. F. BUCK, AND W. L. WILSON

USDOE contract No. DE-AC11-93PN38195.

NOTE

This document is an interim memorandum prepared primarily for internal reference and does not represent a final expression of the opinion of Westinghouse. When this memorandum is distributed externally, it is with the express understanding that Westinghouse makes no representation as to completeness, accuracy, or usability of information contained therein.

NOTICE

BETTIS ATOMIC POWER LABORATORY WEST MIFFLIN, PENNSYLVANIA 15122-0079

Operated for the U.S. Department of Energy
by WESTINGHOUSE ELECTRIC CORPORATION

DISCLAIMER

Laboratory Galling Tests of Several Commercial Cobalt-Free Weld Hardfacing Alloys

B.V. Cockeram, R.F. Buck and W.L. Wilson, Westinghouse-Bettis Atomic Power Laboratory, P.O. Box 79, West Mifflin, PA 15122-0079.

Abstract

Since the mechanical properties of most wear materials are generally insufficient for structural applications, hardfacing alloys have been traditionally weld deposited to provide a wear resistant surface for a base material. An important attribute of a hardfacing alloy that is subjected to high load sliding contact is the resistance to adhesive (galling) damage. Although Co-base hardfacing alloys generally possess excellent galling wear resistance, there is interest in developing cobalt-free replacement hardfacings to reduce radiation exposure costs. A laboratory galling test has been developed for weld hardfacing deposits that is a modification of the standardized ASTM G98-91 galling test procedure. The procedure for testing a weld hardfacing deposit on a softer base metal using a button-on-block configuration is described. The contact stresses for the initiation of adhesive galling damage were measured to rank the galling resistance of several commercial Fe-base, Ni-base and Co-base hardfacing alloys. Although the galling resistance of the Fe-base alloys was generally superior to the Ni-base alloys, neither system approached the excellent galling resistance of the Co-base alloys. Microstructure examinations were used to understand the micro-mechanisms for the initiation and propagation of galling damage. A physical model for the initiation and propagation of adhesive wear is used to explain the lower galling resistance for the Ni-base hardfacings and to understand the influence of composition on the galling resistance of Ni-base alloys. The composition of some Ni base hardfacings was modified in a controlled manner to quantify the influence of specific elements on the galling resistance.

1. Introduction

Since wear resistant materials are generally too brittle for structural applications, the practice of weld depositing a wear resistant hardfacing onto a base metal that possess the needed mechanical properties has been used for many years [1]. Resistance to galling wear damage, which is an extreme form of adhesive surface damage that results from plastic flow or material transfer during metal-to-metal sliding at high loads, is generally desired for most hardfacing alloys. Co-base hardfacing alloys typically possess excellent galling resistance, but normal wear and corrosion produces cobalt debris that become activated and contaminate nuclear power plant components. Replacing the Co-base hardfacing alloys with low cobalt hardfacings would reduce the costs associated with plant contamination and reduce the procurement costs of expensive Co-base weld consumables [2]. A laboratory galling test was developed for hardfacings by modification of the ASTM G98-91 procedure. The results of galling wear testing of hardfacing alloys, and examinations of the wear surfaces and hardfacing microstructures are discussed.

2. Materials

The nominal chemistries for the weld consumables of four commercial Fe-base hardfacings (ELMAX, NoCo-M2, NOREM 02, and Tristelle TS-2), three commercial Ni-base hardfacings (Colmonoy 5, Nucalloy 453, and Nucalloy 488), and one Co-base hardfacing (Stellite 6) are given in Table I. The microstructure of Stellite 6 consists of Co phase dendrites with interdendrite lamella of Cr-rich carbides and Co phase. The hard interdendrite carbides provide a stiff matrix to resist the large amount of plastic deformation that would initiate adhesive damage. The low stacking fault energy (SFE), high work hardening rate, and stress induced phase transformation from face-centered cubic to hexagonal close packed structure at the wear surface are characteristics of the Co phase dendrites that are thought to provide the outstanding galling resistance [1].

The microstructures for NoCo-M2 and NOREM 02 consist of Fe-base dendrites and interdendrite lamella of Cr-rich carbides and Fe phase that are similar in volume fraction to Stellite 6 [2,3,4]. NoCo-M2 and NOREM 02 are slight composition variants of the same family of NOREM alloys. The ELMAX and Tristelle TS-2 microstructures are relatively similar to the NOREM alloys but the volume fractions of interdendrite Cr-rich carbides are much higher. As observed for Stellite 6, the continuous network of interdendrite carbides for the Fe-base hardfacings is thought to provide the rigid alloy matrix that is needed to resist galling damage. The low SFE, oxidation characteristics, and possible austenite to martensite stress induced phase transformation of the Fe phase dendrites at the wear surface are potential mechanisms that provide the good galling resistance of the Fe-base hardfacings.

The microstructure for the Ni-base hardfacings consists of a high volume fraction (40% to 55%) of interdendrite carbides, borides, silicides, and/or combinations of boride/silicide/Ni phase eutectic lamella, and relatively soft Ni phase dendrites [2]. The galling resistance of the Ni-base hardfacings is generally thought to be provided by the high volume fraction of hard interdendrite phases.

3. Experimental Procedure

The hardfacing alloys in Table I were deposited on Type 347 stainless steel bar using a Plasma Transferred Arc Weld (PTAW) process. The hardfacing deposits were applied in two layers to a nominal thickness of 0.4 cm, and the button and block specimens in Fig. 1 were machined from the hardfaced bars. In addition for Colmonoy 5, one set of Colmonoy 5 specimens was machined from hardfaced Alloy 718 bar, and Gas Tungsten Arc Welding (GTAW) was used for two other sets of Colmonoy 5 specimens. The specimens were cleaned in 2-Propanol, acetone, and water, and then individually packaged in polyethylene bags until testing. The block was held in a cup fixture that was typically filled with deionized ambient water, while the hardfaced surface of the button specimen was pressed against the

hardfaced surface of the block. Special fixturing was developed to maintain interfacial and radial alignment between the button and block. A computer-controlled electromechanical load frame was used to apply a constant compressive load on the button, and the test load versus time was recorded during each test. The stress for each galling test was determined from the average load during rotation of the button specimen.

After the desired load was applied and maintained at a consistent value, the button specimen was rotated in a 120° arc ten times within 30 to 90 seconds, which is more severe than the single 360° rotation method that is specified for galling testing in ASTM G98-91 [5]. The 10 X 120° rotation method was adopted because the higher applied stresses for the single 360° rotation method would generally result in excessive yielding of the softer base metal that exceeded the limits of the button specimen design to invalidate the test. After rotation, the specimens were examined both visually and with a 10X eyepiece for signs of adhesive damage and galling. If no galling was observed, the procedure was repeated on a new set of specimens at a higher load. Testing was continued until galling damage was observed. The threshold galling stress (TGS) was then established as the average stress between the highest non-galled stress and the lowest galled stress. Shakedown testing of self-mated Type 316 and 440C stainless steel using a single 360° rotation test was initially done in air in accordance with ASTM G98-91. All of the hardfacing alloys were tested in ambient deionized water, but a few were also tested in air at room temperature. The hardfacings were generally tested as self-mated couples. After testing, selected specimens were sectioned for metallography. The wear surfaces of selected specimens were examined using scanning electron microscopy (SEM) with energy dispersive X-ray (EDX) capability.

4. Galling Test Results

The TGS results for shakedown tests of self-mated Type 316 stainless (6.9 MPa (1.0 ksi)) in air using the single 360° rotation method were equivalent to reported data (6.9 MPa

(1.0 ksi)) [1], which indicates the test method is consistent with previous approaches. Single rotation tests of Type 440C stainless in air (42.1 MPa (6.1 ksi)) and water (248 MPa (36.0 ksi)) bound the reported values for in-air testing of 440C (124 MPa (18 ksi) and 76 MPa (11 ksi)) [5], which demonstrates that differences in surface condition (i.e. cleaning) have a strong influence on TGS. A stringent surface cleaning procedure was used for the specimens tested herein and previous 316 stainless testing, while the cleaning procedure for previous type 440C stainless data is not known. Differences in heat treatment condition may also change the TGS of type 440C stainless steel [5].

The TGS for self-mated Stellite 6 in Fig. 2 was significantly higher than the Fe-base or Ni-base hardfacings. Galling damage could not be produced on Stellite 6 in the more conservative air environment at average contact stresses up to 1,200 MPa (174 ksi). One small galling event was produced during one test at 1,103 MPa in air, but this result was not reproducible. Tests at stresses greater than 1,241 MPa could not be attempted because the button specimen yielded the mating block specimen sufficiently by brinneling to permit contact between the bases of the button and block to invalidate the test. These results agree with a reported TGS of 1,241 MPa ksi for self-mated Stellite 6 in a 5 X 360° rotation test [6].

The TGS values for the Fe-base hardfacings in Fig. 2 were less than Stellite 6, but higher than the TGS values for the Ni-base hardfacings. The TGS determination for the more galling resistance Fe-base hardfacings (NOREM 02 and ELMAX) was somewhat subjective because a well defined stress level for the onset of severe adhesive damage was not easily identified and the TGS was based upon the stress for the onset of severe adhesive damage. The TGS for the Fe-base hardfacings in Fig. 2 generally follow this trend; high Ni contents degrade galling resistance, higher Si, Mn, Co, and N contents improve galling resistance, and high carbon contents increase the volume fraction of Cr-rich carbide precipitates for improved galling resistance [4]. The δ-ferrite content of the hardfacings is also a factor. During early

development of the NOREM hardfacings, the detection of ferromagnetism using a strong magnet was shown to be a sensitive method for identifying δ-ferrite formation in the austenite Fe phase dendrites [3,4]. Examination of the Fe-base galling specimens using a high strength magnet revealed: (1) the strongest magnetism for ELMAX, (2) strong magnetism for NOREM 02, and (3) no magnetism for NoCo-M2 and Tristelle TS-2. Metallography confirmed the presence of a second phase in the ELMAX and NOREM 02 dendrites, which was likely δ-ferrite, while second phase δ-ferrite regions were not detected in NoCo-M2 and Tristelle TS-2 dendrites. The presence of δ-ferrite in the austenite dendrites of ELMAX and NOREM 02 appears to be related to the higher galling resistance. The austenite dendrites of hardfacing alloys that contain δ-ferrite are probably more inclined to undergo a stress induced phase transformation to martensite at the wear surface which may result in improved resistance to adhesive damage or galling. The high cobalt content of the dendrites and higher volume fraction of carbides for Tristelle TS-2 probably improves the adhesion resistance of the microstructure for improved galling resistance.

The lowest TGS values were measured for the Ni-base hardfacing alloys in Fig. 2. Cross-mated tests of Nucalloy 453 and Nucalloy 488 in Fig. 2 resulted in TGS values that were in between the self-mated TGS values. The highest TGS values for the Ni-base hardfacings were measured for Colmonoy 5, but the range of TGS data was also the widest for Colmonoy 5. The use of six different weld consumable chemistries deposited on different base metals, and use of PTAW and GTAW deposition methods contributed to the wide variation of TGS test data for Colmonoy 5. The TGS values for Ni-base hardfacings in Fig. 2 are comparable to previous galling tests of similar Ni-base hardfacings [6,7].

The variation of TGS values with Fe content of the Ni-base weld consumables is shown in Fig. 3. An apparent trend of lower TGS with higher Fe content between the values of 0.25% to 5.5% Fe is shown in Fig. 3. However, the TGS values for two PTAW deposits of

Colmonoy 5 and Nucalloy 453 that were produced by mixing pure Fe powder with pre-alloyed Colmonoy 5 or Nucalloy 453 powder do not fit the trend of TGS versus iron content, which indicates that Fe alone does not explain this trend. Iron additions may slightly decrease the TGS of Ni-base hardfacings from 0.25% to 5.5% Fe, but larger additions of Fe have little influence on the TGS. Similar trends of lower TGS values with higher Cr and lower Ni content in the weld consumables were also observed, but the more sensitive trend was for the Fe content. SEM/EDX examinations have shown that the iron content of the Ni phase is generally a factor of 1.25 to 2 times higher than the nominal Fe content of the hardfacing alloy, and this localization of Fe may contribute to a slight change in TGS with Fe content. Since only slight trends for TGS with Fe, Cr, and Ni composition were observed, a clear and simple composition dependence for the TGS of Ni-base hardfacings has not been defined.

Base metal dilution for the PTAW process is reported to be 5% to 15% [1], and base metal dilution results in a change in the final composition of the hardfacing deposit relative to the weld consumable. Larger additions of Ti and Nb from the base metal to Colmonoy 5 for deposition on Alloy 718 rather than type 347 stainless steel produces differences in the precipitation structure of the Ni phase dendrites that were resolved in a preliminary transmission electron microscopy examination. These differences in Ni phase microstructure that result from deposition on either Alloy 718 or Type 347 stainless probably contribute to the wide differences in TGS in Fig. 3. TGS results in Fig. 3 from three tests of Colmonoy 5 that consisted of a mixed couple of a block specimen with an Alloy 718 base metal and a button specimen with a type 347 stainless base metal (157, 157, 157 MPa) were exactly the same and in between the data for self-mated specimens on Alloy 718 (181 MPa) and 347 stainless (28.3 MPa). The data suggest that two variables may influence the TGS of Ni-base hardfacings: (1) Fe content, and possibly Cr and Ni content of the weld consumable, and (2) base metal composition, which appears to be more potent.

5. Examinations of Ni-base Hardfacing Galling Specimens

A progressively greater amount of surface damage was observed on the Fe-base and Co-base hardfacing specimens as the test stresses were increased to the TGS, and classification of galling was difficult as obvious, severe adhesive damage was not always produced at stress levels above the TGS. TGS determination for the Fe-base hardfacings was based upon the stress that produced a moderate amount of surface damage. In addition to significantly lower TGS values for the Ni-base hardfacings, a sharp transition from minimal surface damage for test stresses just below the TGS to severe adhesive damage and fracture for testing above the TGS was observed. SEM examinations were pursued to gain further insight into this different tribological behavior of Ni-base hardfacings, possibly understand the wide range in TGS values, and determine why the TGS values for Ni-base hardfacings were lower than Fe-base and Co-base hardfacings.

An example of the progression in localized surface damage that illustrates the proposed galling mechanism of Colmonoy 5 is shown in Fig. 4. A transition from light wear to severe wear and adhesion is shown from right to left in Fig. 4. The composition for two locations of obvious smearing (spots #1 and #2), as determined by EDX spot analysis, in the "smearing region" in Fig. 4 are consistent with compositions that were measured for the Ni phase dendrites. The EDX composition of the balled up region in Fig. 4 (spot #3) is also consistent with the Ni phase composition, which indicates that more severe smearing results in the adhesive balling up and tearing away of the Ni phase from the adjacent brittle phases. The brittle matrix phases cannot support the high normal and shear stresses that result from ductile adhesive smearing of the Ni phase, which results in fracture of the adjacent brittle phases, as shown by the fractured debris adjacent to the Ni phase in Fig. 4. More advanced progression of the balling up and tearing away of the Ni phase with more extensive fracture of the brittle phase produces the severe galling damage at the far left in Fig. 4.

Ni-base hardfacings can be characterized as a 40% to 55% volume fraction of brittle carbide, boride, and silicide phases that form an interconnected heterogenous matrix which surrounds the more ductile Ni phase dendrites, as shown by the schematic in Fig. 5a. High stress contact at local asperities during sliding produces some fracturing of the brittle matrix phases, but also results in the adhesive bonding of the Ni phase dendrites shown in Fig. 5b due to the inherently poor galling resistance of Ni-base alloys [1]. Further sliding in Fig. 5c results in smearing, deformation, and agglomeration of Ni phase adhesions and fractured brittle phase debris. Ni phase smearing and fractured brittle phase debris were observed at the Colmonoy 5 wear surface in Fig. 4. The adjacent brittle matrix phases are fractured in Fig. 5c from the high contact stresses that result from adhesive smearing of the ductile Ni phase. Further sliding results in more progressive smearing and the development of high contract stresses at asperities that eventually produce a more severe adhesive event with the balling up of the Ni phase in Fig. 5d, more progressive fracture of the brittle matrix phases, and the initiation of severe galling, as shown in the left-hand side of Fig. 4.

The low galling stresses for Ni-base hardfacings are therefore governed by the stresses at which localized Ni phase adhesion is initiated in combination with the inability of the brittle matrix phases to support the high stresses that are produced by the Ni phase adhesions. The charpy impact toughness for Ni-base hardfacings are less than Fe-base and Co-base alloys [4], but the high volume fraction of brittle matrix phases provide good resistance to surface damage during metal-to-metal sliding when the contact stresses are below the threshold for Ni phase adhesion. The initiation of Ni phase adhesion produces fracturing of the adjacent brittle matrix phases that propagates increased contact stresses and severe surface damage, and these mechanisms accelerate further damage by a self-sustaining snowball effect.

These investigations have shown that the severe galling of Ni phase hardfacings is initiated by Ni phase adhesion. Since examinations have shown that the Fe is preferentially located in the Ni phase and Nb and Ti elements from the base metal are also preferentially dissolved in the Ni phase, both Fe and Nb or Ti likely could have a potent influence on the adhesive tendencies of the Ni phase, which may produce the differences in TGS with Fe content and base metal that were observed in Fig. 3.

6. Summary

The ASTM G98-91 procedure for determination of TGS has been modified for the testing of hardfacing deposits on soft Type 347 stainless base metal by the use of a 10 X 120° rotation method, special alignment fixturing, and continuous maintenance of a constant load. The measured TGS of type 316 stainless steel reference material, and Co-base and Ni-base hardfacings were comparable to reported values. The TGS values for the Co-base hardfacing Stellite 6 were the highest, while the TGS values for Fe-base hardfacings were a factor of 2 to 5 less. The lowest TGS values were observed for Ni-base hardfacings, which is attributed to the adhesive tendencies of the Ni phase dendrites. Examinations have shown that the galling of Ni-base hardfacings is initiated by adhesion of the Ni phase. Segregation of Fe or Ti and Nb into the Ni phase may affect the adhesive tendencies of the Ni phase, which may explain the slight variations of TGS with Fe content of the weld consumable and base metal composition.

Acknowledgements

This work was performed under USDOE Contract No. DE-AC11-93PN38195.

References

[1] Friction, Lubrication and Wear Technology, Materials Handbook, Vol. 18, ASM-I (1992).

[2] S.A. Shiels, W.L. Wilson, K.W. Rosengarth, and G.L. Wire, Proceedings of the Third International Symposium on the Contribution of Materials Investigation to the Reduction of Problems Encountered in Pressurized Water Reactors, Fontevraud, France, September 12-16, 1994. Available as WAPD-T-3032, DOE/OSTI, Oak Ridge TN, 1994.

[3] E.W. Ohriner and E.P. Whelan, Development of Cobalt-Free Hard-facing Alloys for Nuclear Applications: 1984 Progress, EPRI, Palo Alto, California, 1985, NP-4237.

[4] E.K. Ohriner, T. Wada, E.P. Whelan, and H. Ocken, Met. Trans., 22A (1991) 983.

[5] Standard Test Method for Galling Resistance of Materials, G98, Annual Book of ASTM Standards, Vol. 03.02, ASTM, 1992.

[6] A.K. Velan, Laboratory Evaluations of Cobalt-Free, Nickel-Based Hard-Facing Alloys for Nuclear Applications, EPRI, Palo Alto, California, 1987, NP-4993.

[7] W.B. Burdett, Proceedings of the Japan International Tribology Conference, Nagoya, Japan, 1990, p. 707.

TABLE I. NOMINAL COMPOSITIONS OF WELD CONSUMABLES FOR VARIOUS COMMERCIAL HARDFACING ALLOYS

ALLOY	COMPOSITION (Wt %)												HARD-NESS (HRC)
	Fe	Ni	Cr	C	Si	Mn	Mo	N	V	W	B	Co	
Co-base Alloy													
Stellite 6[1]	3.0	1.0	28.0	1.0	1.0	–	–	–	–	5.0	–	Bal	46
Ni-base Alloys													
Colmonoy 5[2]	3.7	BAL	12.0	0.6	3.7	–	–	–	–	–	2.5	–	45-50
Nucalloy 453[1]	3.0	BAL	10.0	0.85	5.3	–	–	–	–	2.0	0.5	–	43
Nucalloy 488[1]	5.5	BAL	17.5	0.3	6.8	–	–	–	–	1.0	1.0	–	45
Fe-base Alloys													
NoCo-M2[1]	BAL	8.0	25.0	0.9	3.0	5.0	2.0	0.15	–	–	–	–	32-36
NOREM 02[1]	BAL	4.0	25.0	1.2	3.3	4.5	2.0	0.16	–	–	–	–	36
ELMAX[3]	BAL	–	17.0	1.7	0.4	0.3	1.0	–	3.0	–	–	–	49-52
Tristelle TS-2[1]	BAL	10.0	35.0	2.0	5.0	–	–	–	–	–	–	12.0	40-42

1 Tradename of Stoody Deloro Stellite Div. of Thermodyne Industries.
2. Tradename of Wall Colmonoy Corp., Madison Heights, MI.
3. Tradename of Uddeholm Corporation, Rooling Meadows, Ill.

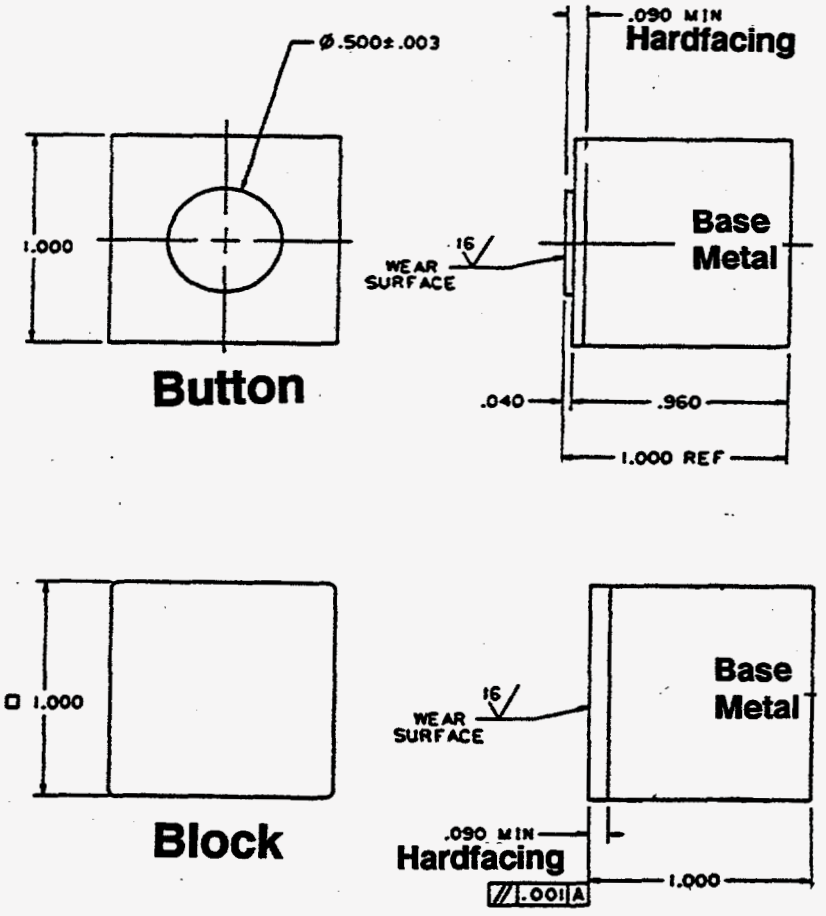

Fig. 1. Schematic of the button and block hardfacing galling specimens.

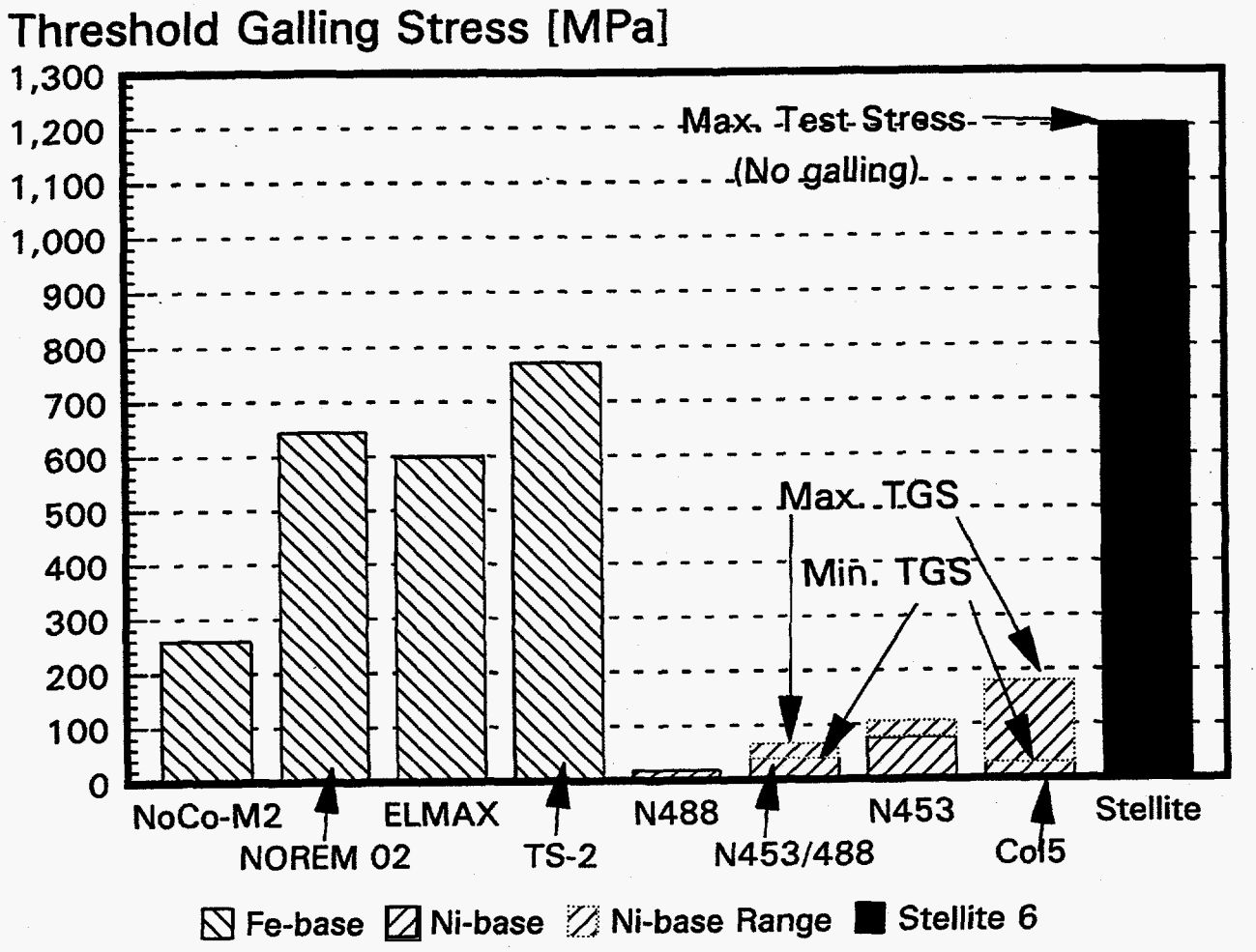

Fig. 2. Summary of threshold galling stress values for various Fe-base and Ni-base hardfacing alloys and the Co-base hardfacing alloy Stellite 6. With the exception of the Nucalloy 453/Nucalloy 488 couples, all hardfacings were tested self-mated. Stellite 6 was tested in ambient air, and all other hardfacings were tested in ambient water. Multiple tests were performed on Colmonoy 5, Nucalloy 453, and the Nucalloy 488/Nucalloy 488 couples to give the indicated range in TGS values, but one TGS value was determined for NoCo-M2, NOREM 02, ELMAX, TS-2, Nucalloy 488, and Stellite 6.

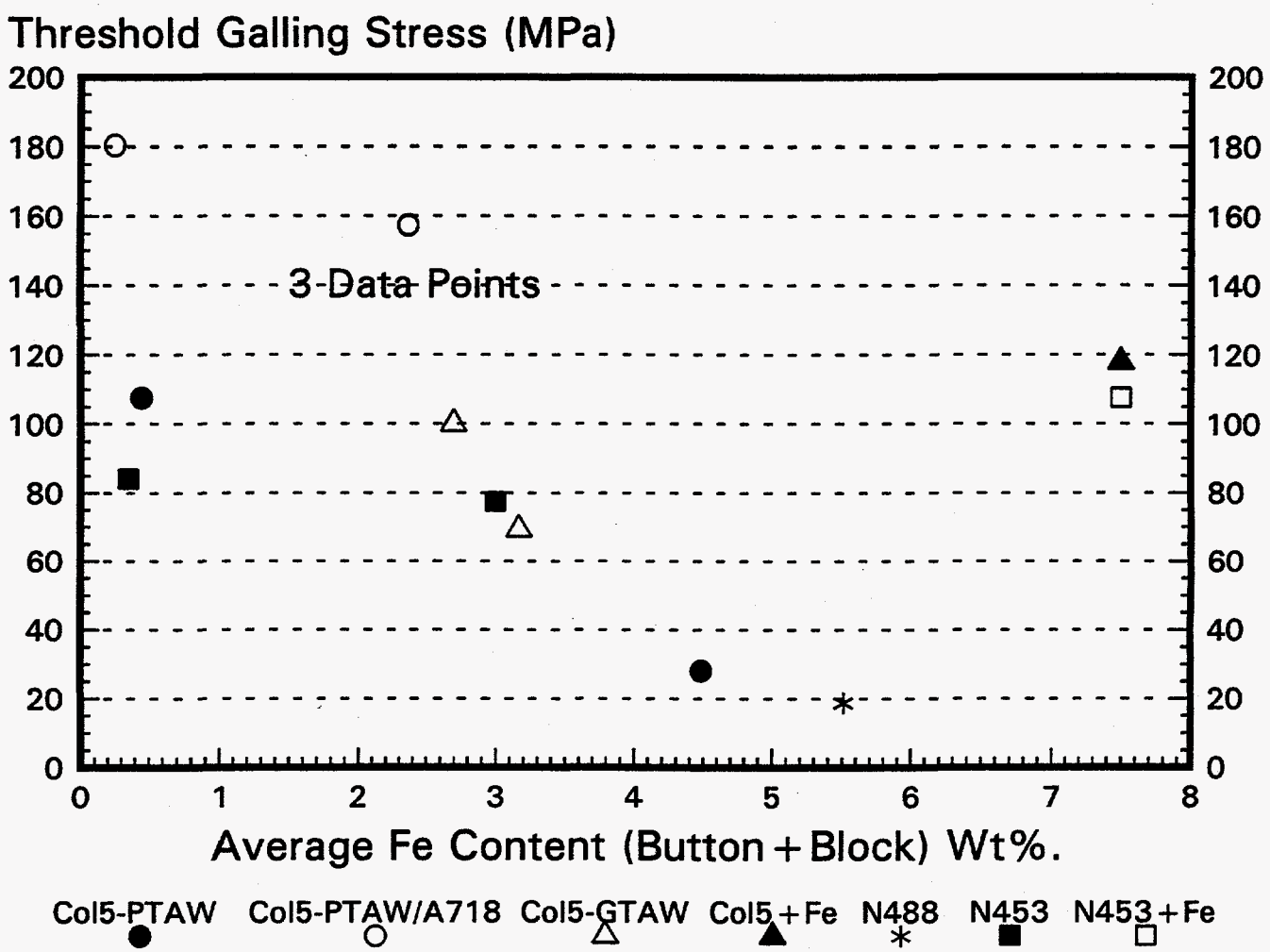

Fig. 3. Plot of threshold galling stress versus the Fe content of the weld consumable for self-mated tests of Ni-base hardfacings in ambient water. With the exception of a few Colmonoy 5 deposits on Alloy 718 (Col5-PTAW/A718), all deposits were made on Type 347 stainless steel. The data labeled 3 points are the repeated TGS values for a mixed Colmonoy 5 couple of Colmonoy 5 deposited on Alloy 718 (blocks) and Type 347 stainless (buttons). Deposits of Colmonoy 5 (Col5+Fe) and Nucalloy 453 (N453+Fe) were produced by mixing prealloyed powder with pure Fe powder.

INTENTIONALLY BLANK

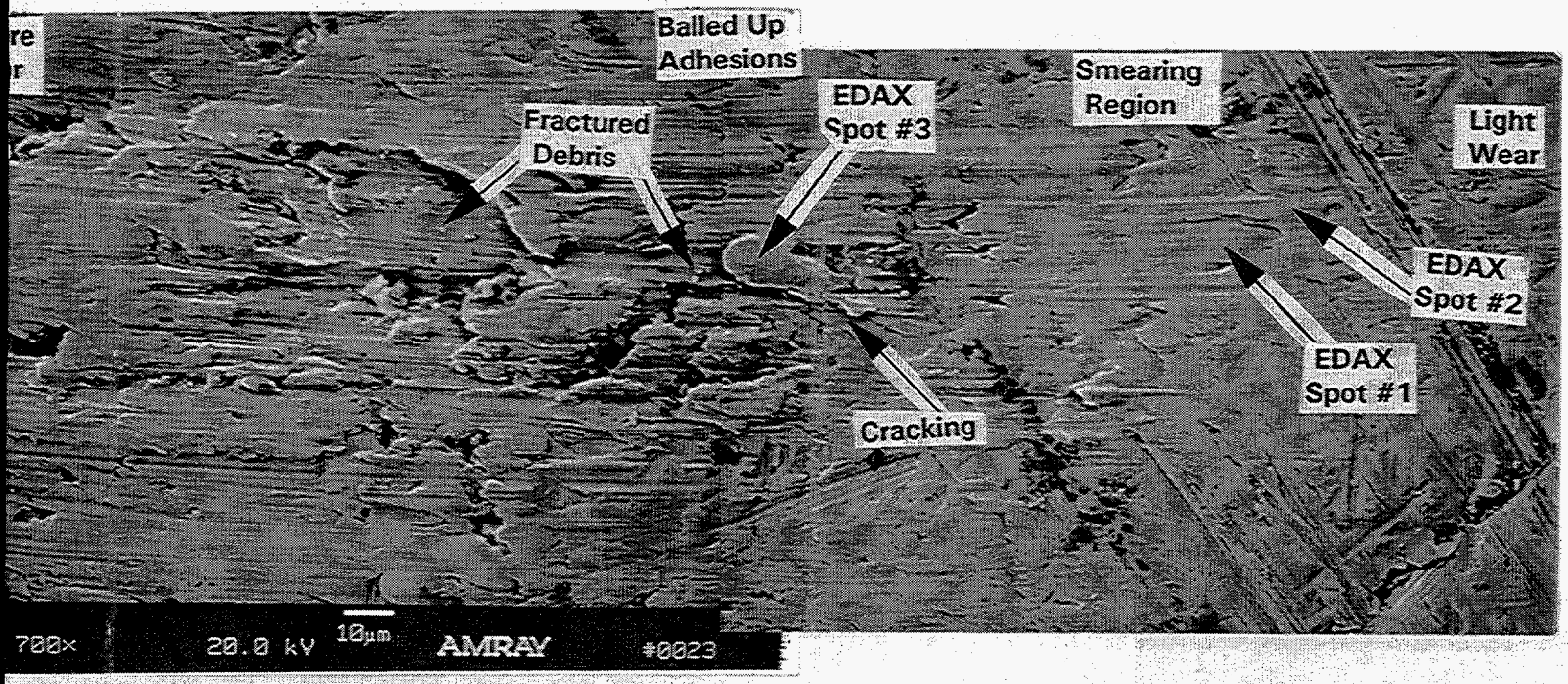

EDX CHEMISTRY RESULTS OF SPOTS IN THE ABOVE SEM MICROGRAPH
(in Atomic%)

Area in Micrograph	Ni	Cr	Fe	Si	O
Spot 1	82	9	1	8	--
Spot 2	88	7	1	4	--
Spot 3	84	9	1	6	--

Fig. 4. SEM/BSE images that show smearing and initiation of galling on a self-mated Colmonoy 5 block specimen at 700X magnification with EDX spots.

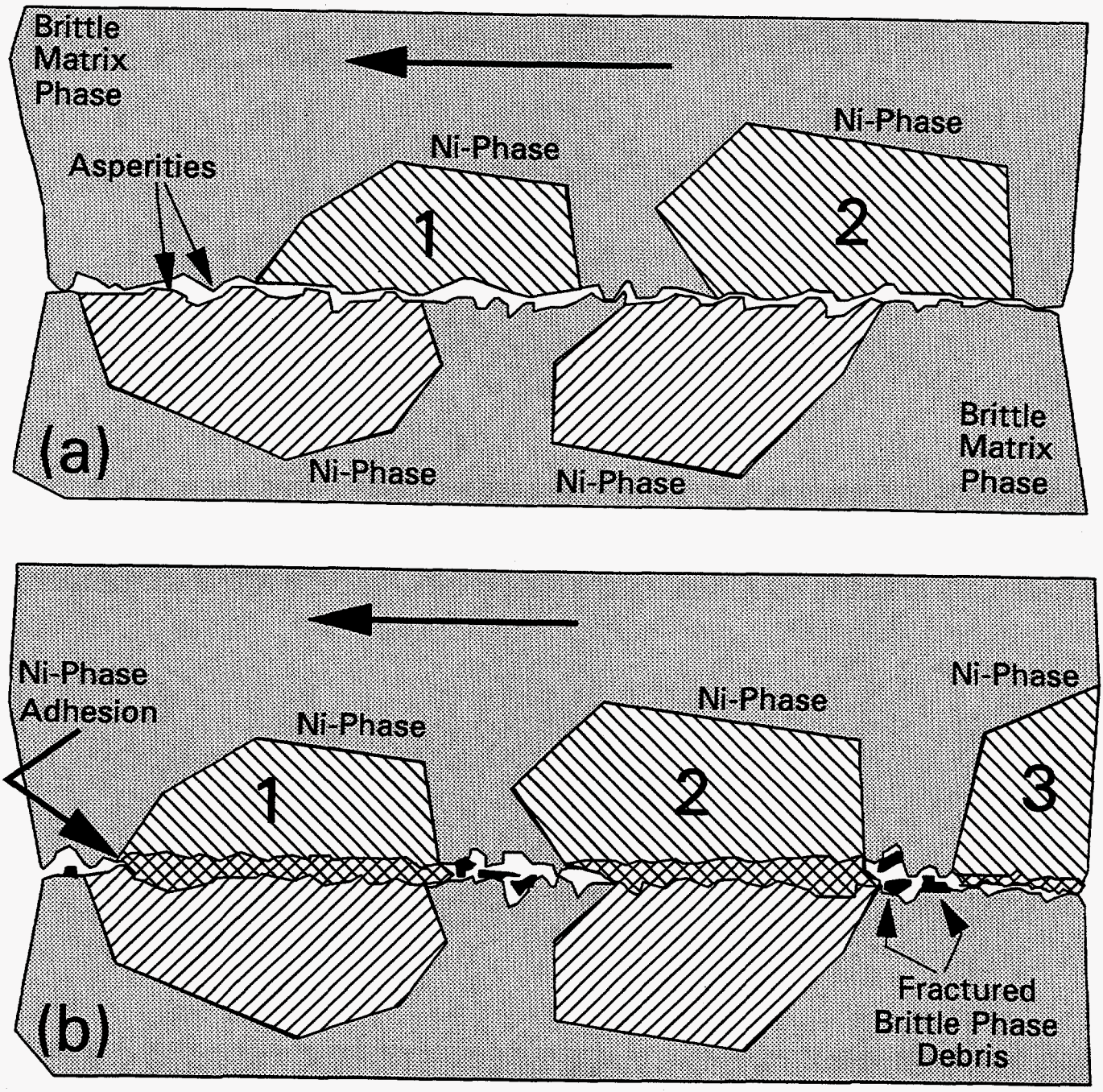

Fig. 5. Schematic representations for the initiation of the galling of self-mated Colmonoy 5 with the arrow identifying the direction of sliding motion; the bottom surface is stationary (block) while the top surface moves (button): (a) initial surface of self-mated Colmonoy 5 with the Ni phase (cross-hatched) and brittle matrix of carbide, boride and silicide phases (light shading), (b) some sliding movement of the top surface with the imitation of adhesion at the Ni phase regions (double cross-hatch) and fracture of brittle phase adhesions to produce brittle phase debris (black shading), (c) further movement with Ni phase adhesion, smearing and fracturing of the adjacent brittle matrix, and (d) further sliding produces more progressive adhesive damage by the balling up of the wear debris with increased brittle phase fracturing, which gives the severe galling of Colmonoy 5.

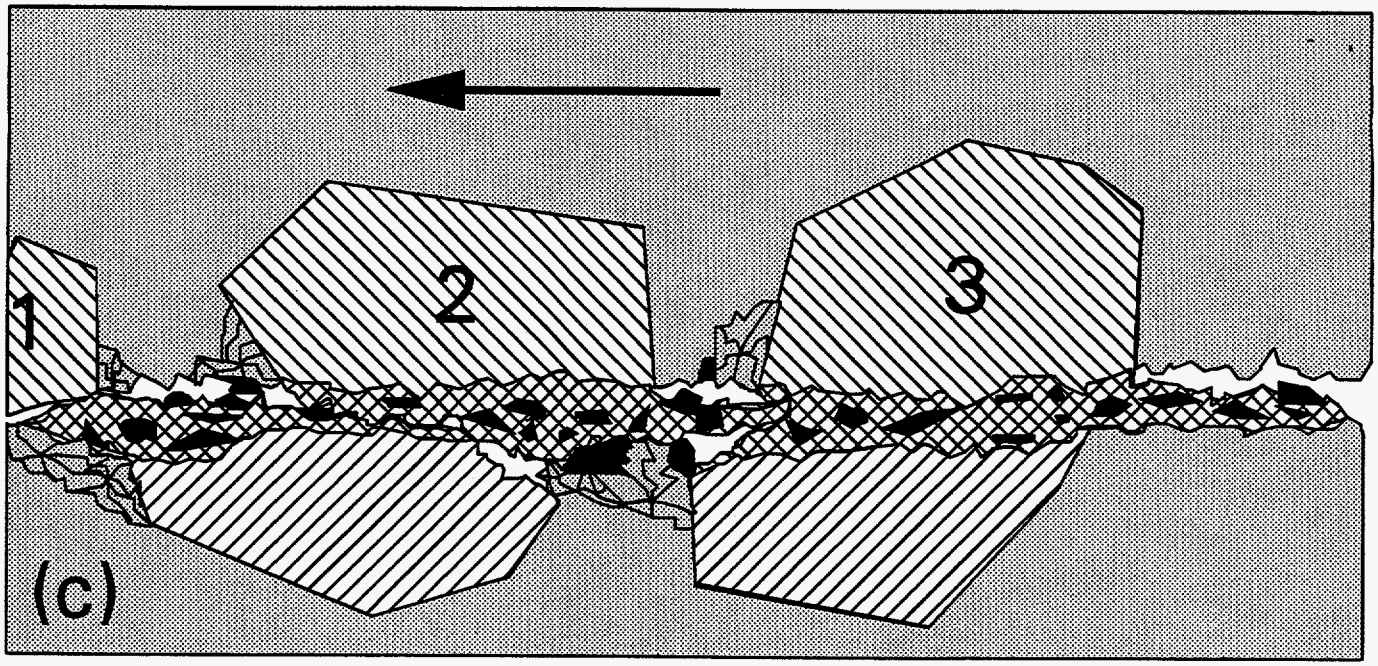

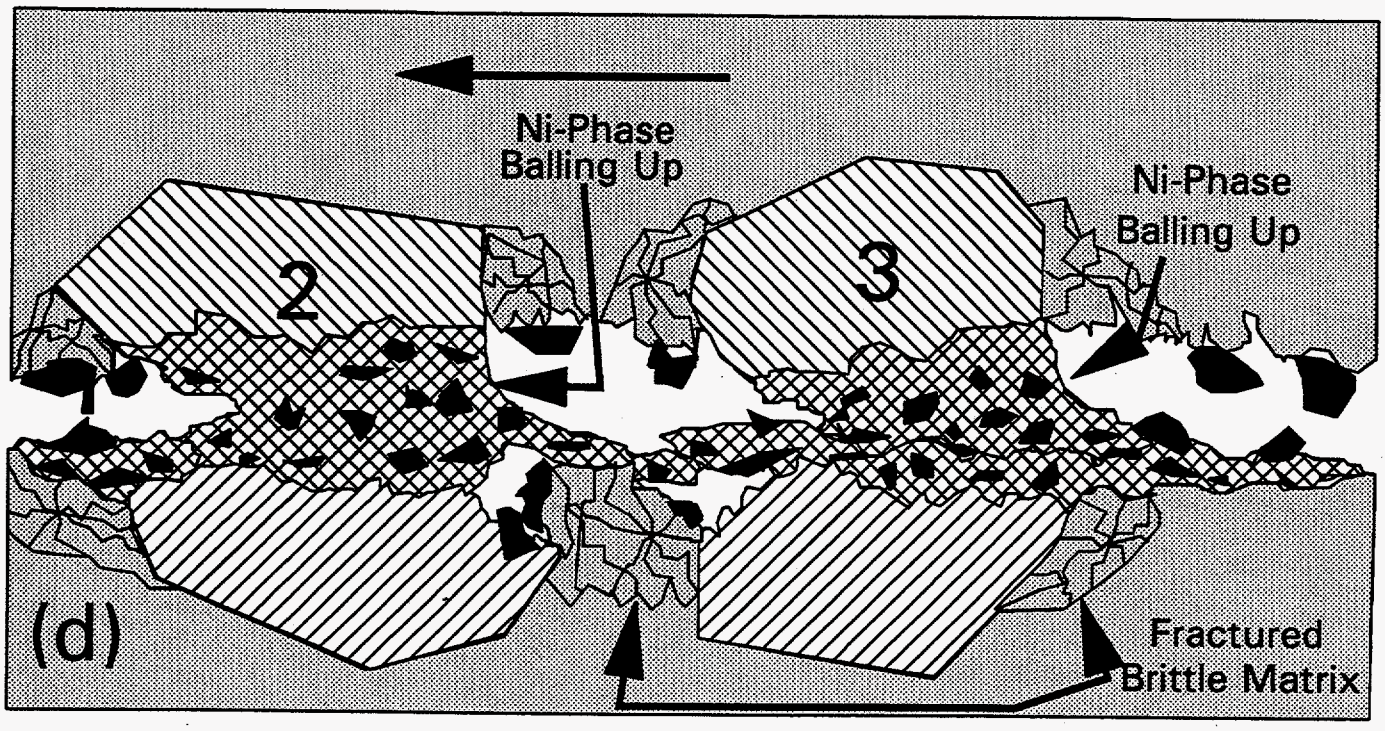

Fig. 5. Continued.